ＩＳＳＮ１３４６－７８３２

独立行政法人港湾空港技術研究所

港湾空港技術研究所報告

REPORT OF THE PORT AND AIRPORT RESEARCH INSTITUTE

VOL.49　NO.2　June 2010

NAGASE, YOKOSUKA, JAPAN

INDEPENDENT ADMINISTRATIVE INSTITUTION,
PORT AND AIRPORT RESEARCH INSTITUTE

港湾空港技術研究所報告（REPORT OF PARI）

第 49 巻　第 2 号（Vol. 49，No. 2），　2010年6月（June 2010）

目　　次（CONTENTS）

REPORT OF THE PORT AND
AIRPORT RESEARCH INSTITUTE
Vol.49, No.2 (June 2010)

Numerical Simulation of Cyclic Seaward Bar Migration

Yoshiaki KURIYAMA*

Synopsis

A one-dimensional model for beach profile change was developed to predict cyclic longshore bar evolutions. The cross-shore sediment transport was assumed to be composed of suspended load due to wave breaking and bed load due to velocity skewness, velocity atiltness, and beach slope. The model was calibrated with beach profile data obtained every weekday at 5-m intervals along a 400-m-long pier at the Hazaki Oceanographical Research Station, located on the Hasaki coast of Japan, during a 1-year period from January to December 1989. The optimal values of the parameters included in the cross-shore sediment transport rate formula and the smoothing number for suspended load were obtained so that the error function that was the sum of the errors in elevation and bar crest position was minimal. The model with the optimal parameter set and the optimal smoothing number was applied to the bar migrations during a period of 2 years, including the 1-year calibration period of 1989 and the following year of 1990. The predicted bar crest positions agreed well with the measured positions, and the Brier skill score was over 0.5 in the bar-trough zone at the end of the 2-year calculation. The model was also applied to bar evolutions outside the calibration period, during the period from 1991 to 2000, which was divided into five 2-year blocks. With the exception of the block representing 1999 to 2000, the model qualitatively reproduced cyclic bar migrations.

Key Words: bar migration, bar evolution, bed load, cross-shore sediment transport, longshore bar, numerical model, suspended load

* Head, Coastal Sediments and Processes Group, Marine Environment and Engineering Department
Nagase 3-1-1, Yokosuka, Kanagawa 239-0826, Japan
Phone : +81-46-844-5045 Fax : +81-46-841-9812 e-mail: kuriyama@pari.go.jp

港湾空港技術研究所報告
第 49 巻第 2 号(2010. 6)

沿岸砂州の繰り返し沖向き移動に関する数値計算

栗山　善昭*

要　　旨

沿岸砂州の繰り返しの沖向き移動を推定するために，断面変化に関する数値シミュレーションモデルを構築した．モデルは砕波によって浮遊した底質が戻り流れにより沖向きに輸送される浮遊砂量および流速の非線形性による岸向きの掃流砂量，海底勾配による掃流砂量を考慮している．モデルに含まれる漂砂量の係数を，茨城県波崎海岸でほぼ毎日観測された 1989 年の 1 年間の断面変化を基に決定するとともに，モデルの現地適用性をキャリブレーション期間を含む 1989 年～1990 年の 2 年間およびそれ以外の期間である 1991 年～2000 年の 10 年間の現地データで検証した．その結果，モデルはキャリブレーション期間を含む約 2 年間の繰り返しの沖向き移動を定量的に再現でき，それ以外の期間についても，定性的には繰り返しの砂州移動を再現できた．

キーワード：沿岸砂州，砂州移動，岸沖漂砂量，浮遊砂，掃流砂，数値モデル

＊ 海洋・水工部　沿岸環境領域　沿岸土砂管理研究チーム
〒239-0826　横須賀市長瀬3-1-1　独立行政法人　港湾空港技術研究所
電話：046-844-5045　Fax：046-841-9812　　e-mail: kuriyama@pari.go.jp

CONTENTS

1. Introduction

Longshore bars are frequently observed on sandy beaches, and migrate seaward and shoreward in the short term (shorter than several weeks). However, medium-term (several weeks to 10 years) and long-term (longer than 10 years) bar migrations are more frequently in the seaward direction (e.g., Birkemeier, 1984; Lippmann et al., 1993; Ruessink and Kroon, 1994; Wijnberg and Terwindt, 1995; Shand and Bailey, 1999; Shand et al., 1999; Kuriyama, 2002; Ruessink et al., 2003; Kuriyama et al., 2008a).

Bars significantly influence currents and morphological variations in the nearshore zone. Although the shoreline normally retreats during a storm and recovers after the storm, laboratory experiments by Yamamoto and Sato (1998) demonstrated that the shoreline did not recover during a mild wave condition when the offshore bar formed during the preceding severe wave condition was removed. Coastal ecological systems are also influenced by bars. Higano (1994) showed that the predominant species of bivalves differ on the shoreward and seaward sides of a longshore bar. Therefore when we deal with morphological and ecological problems of sandy beaches, predicting bar migrations is strongly required.

To simulate medium-term bar migrations, numerous models have been proposed. Some of the models could predict a part, or in some cases the whole, cycle of bar evolution consisting of generation, seaward migration and decay. However, the durations of bar evolution cycles are longer than the periods investigated when testing model validity; therefore, the ability of models to reproduce cyclic bar evolutions has not been fully examined. The objective of this study was to develop a process-based one-dimensional model for beach profile change and to investigate the validity of the simulated cyclic bar evolutions using daily field measurements of beach profiles.

2. Previous studies

A model for predicting the locations of bar crest was developed by Plant et al. (1999), who assumed that a bar migrates toward a wave height-dependent equilibrium point and that the migration rate is proportional to the wave height and the distance between the present bar crest location and the equilibrium one. They applied their model to bar migration at Duck, North Carolina, USA, and showed that the model successfully predicted bar migration over an interval of 7 years. The model was expanded by Pape et al. (2009a), who demonstrated that the model reasonably reproduced bar crest movements over an interval of about 8 years at the Gold Coast, Australia, and Egmond, the Netherlands.

Pape et al. (2007) and Pape et al. (2009b) developed another model for bar crest movement using a neural network. The model worked well for bar crest movement on the Gold Coast over about 2 years. However, on the Hasaki coast, Japan, where the duration of seaward bar migration is about 1 to 2 years, while some of the bar crest movements were predicted well by the model, some others were not, and the overall model performance over an interval of 15 years was concluded to be relatively poor.

A method of predicting not only the bar crest position but also bar evolution is to estimate the elevation change on the basis of the spatial gradient of the cross-shore sediment transport rate. Gallagher et al. (1998) predicted bar migration at Duck over about 2 months using the cross-shore sediment transport rate formula proposed by Bailard (1981) and substituting velocities measured in the field into the formula. The result showed that seaward bar migration was predicted well using this method but that the shoreward migration was not. Hoefel and Elgar (2003) improved the model by adding a term related to the acceleration skewness and successfully reproduced both seaward and shoreward bar migrations.

Plant et al. (2004) developed a process-based model in which the cross-shore sediment transport rate was assumed to be a quadratic function of the wave height to water depth ratio as in the earlier study of Plant et al. (2001). The model was applied to a bar migration at Duck over about 1 month, but the model performance was relatively poor. Marino-Tapia et al. (2007a) predicted bar migrations at Duck using Bailard's (1981) cross-shore sediment transport rate formula and substituting the shape functions developed by Mario-Tapia et al. (2007b) into the terms of the third and fourth power of velocity. The bar crest movement predicted by the model for a 77-day interval fitted that measured in the field reasonably well.

van Rijn et al. (2003) compared short- and medium-term beach profile changes measured on a barred beach at Egmond with those predicted by several process-based models. They showed that the two models, UNIBEST and CROSMOR, worked well for the outer bar migration over about 4 months but not for inner bar migration and the beach profile change in

the foreshore.

Using the UNIBEST model, Ruessink et al. (2007) successfully reproduced bar migrations at Hasaki, Duck and Egmond over intervals of 10 days to 4 months. Furthermore, Ruessink and Kuriyama (2008) investigated the performance of the UNIBEST model for bar migration at Hasaki over 18 months; the results showed that the performance of this model was high for the first 15 months but rapidly decreased after this time. Pape et al. (2009b) also investigated the performance of the UNIBEST model for bar migration at Hasaki during the period from 1987 to 2001, which was divided into 16 blocks, each of which included a series of bar migrations. The results showed that even with optimal parameter sets for each block, the model performance was variable with some poor results. Walstra and Ruessink (2009) demonstrated that the UNIBEST model predicted the bar development and decay at Noordwijk, the Netherlands, over 3 years, although the field data used for the model validation were not obtained for the same interval as the prediction.

3. Data description

The model developed in this study was compared with beach profile data obtained at Hazaki Oceanographical Research Station (HORS). HORS is located on the Hasaki coast of Japan facing the Pacific Ocean (**Figure 1**) and has a 400-m-long pier. The beach profiles along the pier have been measured every weekday at 5-m intervals since 1986 using a 5-kg lead weight from the pier and a level and staff shoreward of the pier. The median sediment diameter along the profile is 0.18 mm, and it remains almost uniform along the profile (Katoh and Yanagishima, 1995). The bathymetry around the pier is almost uniform alongshore according to Kuriyama (2002), who applied Empirical Orthogonal Function analysis to 17 bathymetric maps around HORS obtained from 1986 to 1998. Based on the datum level at Hasaki (Tokyo Peil -0.687 m), the high, mean and low water levels are 1.25 m, 0.65 m, and -0.20 m, respectively, and the tidal range is 1.45 m. Wind angle and velocity were measured at the tip of the pier for 10 minutes every hour. Deepwater waves were measured at a water depth of about 24 m with an ultrasonic wave gage for 20 minutes every 2 hours (see location on **Figure 1**).

Figure 2 shows the mean beach profiles during the period from 1987 to 2001. Each position along the pier is referred to by its seaward distance relative to the reference point located

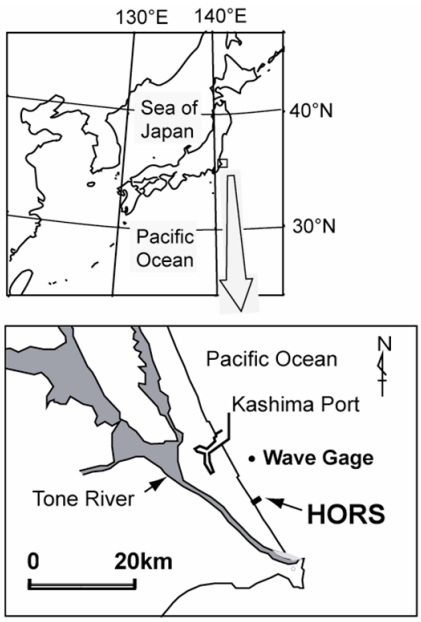

Figure 1 Locations of HORS and the wave gage.

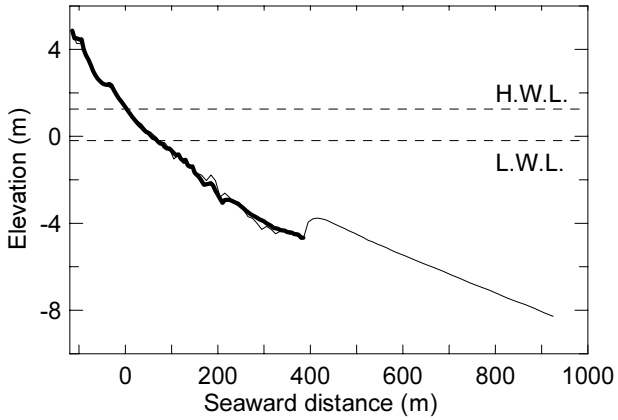

Figure 2 Mean beach profile from 1987 to 2001 based on daily measurements along the HORS pier (thick line) and yearly bathymetric surveys around HORS (thin line). The elevation is based on the Hasaki datum level.

close to the pier entrance and designated as "P." For example, P230m denotes a position 230 m seaward from the reference point. The mean beach slope decreases gradually offshore. Gradients are about 1/40 near the shoreline at the low water level, about 1/80 at P250m, and about 1/110 near the tip of the pier. Longshore bars are frequently observed in the area between P180m and P380m, and they move seaward with durations of 1 to 2 years (Kuriyama et al., 2008a).

4. Numerical model

The one-dimensional numerical model for bar evolution developed in this study is composed of five sub-models for wave and surface roller transformation, undertow velocity, longshore current velocity, velocity skewness and atiltness, and beach profile change. The sub-models for wave and surface roller transformation, undertow velocity and longshore current velocity are based on those of Kuriyama (2010a).

4.1 Wave and surface roller transformation

The wave and surface roller transformation sub-model estimates the cross-shore variation of the root-mean-square wave height H_{rms}, which is used in estimating the undertow and longshore current velocities and sediment transport rates in the following sub-models. A Rayleigh distribution is assumed as the wave height probability density function over an entire computational domain, following Thornton and Guza (1983). The energy of waves with heights larger than the breaking wave height is dissipated.

The breaking wave height is estimated with Equation (1), as proposed by Seyama and Kimura (1988).

$$\frac{H_b}{h_b}=C_{br}\left[0.16\frac{L_0}{h_b}\left\{1-\exp\left[-0.8\pi\frac{h_b}{L_0}\left(1+15\tan^{4/3}\beta\right)\right]\right\}-0.96\tan\beta+0.2\right] \tag{1}$$

where H_b is the breaking wave height, h_b is the breaking water depth, C_{br} is a nondimensional coefficient, L_0 is the offshore wavelength and tanβ is the beach slope. The nondimensional coefficient C_{br} was introduced by Kuriyama (1996) to fit experimental data-based Equation (1) to field data. The beach slope is defined as positive for water depth increasing seaward and estimated as the average slope in a 30-m-long region for which the definition point is located at the center.

Wave energy dissipation is estimated using the periodic bore model proposed by Thornton and Guza (1983) and 20 representative wave heights raging from H_b to $3H_b$.

$$\frac{\partial E_W C_g\cos\theta}{\partial x}=\int_{H_b}^{\infty}P(H)B(H)dH$$
$$B(H)=\frac{1}{4}\rho g\frac{1}{T}\frac{(B_W H)^3}{h} \tag{2}$$

where E_w is the wave energy, C_g is the group velocity, θ is the wave direction, x is the seaward distance, $P(H)$ is the probability density of the wave height, ρ is the seawater density, g is the gravitational acceleration, T is the wave period, H is the wave height and h is the water depth. A nondimensional parameter B_w was formulated as in Equation (3) of Kuriyama and Ozaki (1996) using Seyama and Kimura's (1988) experimental data.

$$B_W=C_B\left\{1.6-0.12\ln(H_0/L_0)+0.28\ln(\tan\beta)\right\} \tag{3}$$

where H_0 is the offshore wave height and C_B is a nondimensional coefficient.

The calculation uses the peak wave period as the wave period, following Grasmeijer and Ruessink (2003). The significant wave height $H_{1/3}$ is estimated as $H_{1/3} = 1.416\ H_{rms}$.

The development and decay of a surface roller in the surf zone is estimated on the basis of the energy balance following Kuriyama (2010a), who assumed that the vertical distribution of the cross-shore velocity in a surface roller is triangular with the celerity C at the top of the roller and zero at the bottom, as described by Kuriyama and Nakatsukasa (2000).

$$\frac{\partial(E_W C_g\cos\theta)}{\partial x}+\frac{\partial(F_r\cos\theta)}{\partial x}=D_r,\quad F_r=\frac{1}{8}\rho C^3\frac{A_r}{L}$$
$$D_r=B_r\frac{gF_r}{C^2}\frac{A_r}{h^2} \tag{4}$$

where F_r is the surface roller energy flux, D_r is the energy dissipation rate of a surface roller, A_r is the area of a surface roller and B_r is a nondimensional coefficient, which was set to be 0.096 according to Kuriyama (2010a).

4.2 Undertow velocity

The vertically averaged undertow velocity U is estimated from Equation (5) from Svendsen (1984).

$$U=\frac{Q_w+Q_r}{d_{tr}} \tag{5}$$

where Q_w and Q_r are the mass fluxes due to waves and surface rollers, respectively. The value of d_{tr} represents the distance between the wave trough level and the bottom, and is assumed to be $d_{tr} = h - H/2$.

Equation (6), which was also proposed by Svendsen (1984), is used to estimate Q_w.

$$Q_W=\frac{C}{h}\zeta_{rms}^2 \tag{6}$$

where ζ_{rms} is the standard deviation of the water surface elevation of a wave, which is obtained from Equation (7) with

the parameter Π for wave nonlinearity proposed by Goda (1983).

$$\zeta_{rms} = \frac{1}{2\sqrt{2}} H_{rms}, \qquad \Pi < 0.15$$

$$\zeta_{rms} = \frac{1}{1.668 \log_{10} \Pi_{rms} + 4.204} H_{rms}, \quad 0.15 \le \Pi < 3$$

$$\zeta_{rms} = \frac{1}{5} H_{rms}, \qquad \Pi \ge 3 \tag{7}$$

$$\text{with} \quad \Pi = \frac{H_{rms}}{L} \tanh^3 \frac{2\pi h}{L} \tag{8}$$

where L is the wavelength.

The value of Q_r is estimated as follows:

$$Q_r = \frac{A_r C}{2L} \tag{9}$$

4.3 Longshore current velocity

The vertically averaged longshore current velocity V is estimated from Equation (10), which represents the momentum balance among the gradient of the radiation stress R_x, the wind stress W_x, the gradient of the momentum flux due to a surface roller M_x, the lateral mixing term L_x and the bottom friction F_x.

$$R_x - W_x + M_x - L_x + F_x = 0 \tag{10}$$

The gradient of the radiation stress term R_x is estimated using small-amplitude wave theory.

$$R_x = \frac{1}{\rho h} \left(\frac{\partial S_{yx}}{\partial x} \right), \quad S_{yx} = \rho g \frac{C_g}{C} \frac{1}{8} H_{rms}^2 \cos\theta \sin\theta \tag{11}$$

The wind stress W_x is assumed to be

$$W_x = \frac{1}{\rho h} C_d \rho_a W_v^2 \sin\alpha_w \tag{12}$$

where C_d is a nondimensional coefficient, ρ_a is the air density, W_v is the wind velocity, and α_w is the wind direction. The value of C_d was assumed to be 0.0022 following Kuriyama et al. (2008b).

The gradient of the momentum flux due to a surface roller M_x is expressed as

$$M_x = \frac{1}{\rho h} \left(\frac{\partial M_r}{\partial x} \right), \quad M_r = -\frac{1}{3} \rho_w C^2 \frac{A_r}{L} \cos\theta \sin\theta \tag{13}$$

The lateral mixing term L_x is assumed, as in the study of Ruessink et al. (2001), with a dimensional coefficient ν.

$$L_x = \frac{\partial}{\partial x} \left(\varepsilon \frac{\partial V}{\partial x} \right), \quad \varepsilon = \nu h \tag{14}$$

The bottom friction F_x, as proposed by Nishimura (1988), is used in the model.

$$F_x = \frac{C_f}{h} (W + \frac{w_b^2}{W} \sin^2\theta) V$$

$$W = \frac{\sqrt{V^2 + w_b^2 + 2Vw_b \sin\theta} + \sqrt{V^2 + w_b^2 - 2Vw_b \sin\theta}}{2}$$

$$w_b = \frac{2v_m}{\pi}, \quad v_m = \frac{\pi H_{rms}}{T \sinh(\frac{2\pi h}{L})} \tag{15}$$

where C_f is a nondimensional coefficient and $u_{b,rms}$ is the amplitude of orbital near-bottom velocity. Following Garcez-Faria et al. (1998) and Ruessink et al. (2001), the friction coefficient C_f is assumed to be a function of the water depth as expressed by Equation (16) with the apparent bed roughness k_a.

$$C_f = 0.015 \left(\frac{k_a}{h} \right)^{1/3} \tag{16}$$

4.4 Velocity skewness and atiltness

In the beach profile change sub-model mentioned later, velocity and acceleration asymmetries are taken into account although the wave and surface roller transformation sub-model mentioned above cannot predict their properties. Hence, this section discusses how to estimate the velocity and acceleration asymmetries.

As parameters representing the velocity and acceleration asymmetries, velocity skewness $\left(\sqrt{\beta_1}\right)_u$ and velocity atiltness $(\beta_3)_u$, which was proposed by Goda (1985), were chosen.

$$\left(\sqrt{\beta_1}\right)_u = \frac{\frac{1}{N}\sum_{i=1}^{N} \left(u_i - \bar{u}\right)^3}{u_{rms}^3}, \quad u_{rms} = \frac{1}{N}\sum_{i=1}^{N} \left(u_i - \bar{u}\right)^2 \tag{17}$$

$$\left(\beta_3\right)_u = \frac{\frac{1}{N-1}\sum_{i=1}^{N-1} \left(a_i - \bar{a}\right)^3}{a_{rms}^3}, \quad a_i = \frac{u_{i+1} - u_i}{\Delta t}$$

$$a_{rms} = \frac{1}{N-1}\sum_{i=1}^{N-1} \left(a_i - \bar{a}\right)^2 \tag{18}$$

where u is the fluid velocity, a is the acceleration and N is the data number. The overbar denotes the average value.

On the basis of fluid velocities measured in the surf zone at HORS, Kuriyama et al. (1990) and Kuriyama (1991) proposed Equations (19) and (20) for estimating velocity skewness and atiltness from $\Pi_{1/3}$, which is a wave

nonlinearity parameter proposed by Goda (1983) and is a function of the wave height, wavelength, and water depth (Equation (21)).

$$\begin{aligned}\left(\sqrt{\beta_1}\right)_u &= 3.37\log\Pi_{1/3} + 0.51, \quad 0.1 \le \Pi_{1/3} < 0.4\\ \left(\sqrt{\beta_1}\right)_u &= 0.36, \qquad\qquad 0.4 \le \Pi_{1/3} < 2\end{aligned} \tag{19}$$

$$\left(\beta_3\right)_u = 1.03\Pi_{1/3} + 0.76, \qquad 0.3 \le \Pi_{1/3} < 2 \tag{20}$$

$$\Pi_{1/3} = \frac{H_{1/3}}{L_{1/3}}\coth^3\frac{2\pi h}{L_{1/3}} \tag{21}$$

where $L_{1/3}$ is the wavelength corresponding to the significant wave period.

Goda (1983) showed that the skewness of surface waves is proportional to $\Pi_{1/3}$ when $\Pi_{1/3}$ < 0.15. Doering and Bowen (1995) proposed formulae for estimating wave skewness and asymmetry using the Ursell parameter. On the basis of these findings, $\left(\sqrt{\beta_1}\right)_u$ and $(\beta_3)_u$ were assumed to be expressed by Equations (22) and (23), respectively, and the coefficients of c_1 to c_5 were determined so that Equations (22) and (23) fit well with Equations (19) and (20), respectively.

$$\begin{aligned}\left(\sqrt{\beta_1}\right)_u &= c_1\Pi_{1/3}, \qquad\qquad \Pi_{1/3} < 0.15\\ \left(\sqrt{\beta_1}\right)_u &= \left[c_2 + c_3\log(\frac{3\pi}{4}\Pi_{1/3})\right]\\ &\cos\left\{\left[-90 + 90\tanh(0.73\frac{4}{3\pi\Pi_{1/3}})\frac{\pi}{180}\right]\right\}, \quad 0.15 \le \Pi_{1/3}\end{aligned} \tag{22}$$

$$\begin{aligned}\left(\beta_3\right)_u &= \left[c_4 + c_5\log\log(\frac{3\pi}{4}\Pi_{1/3})\right]\\ &\cos\left\{\left[-90 + 90\tanh(0.73\frac{4}{3\pi\Pi_{1/3}})\frac{\pi}{180}\right]\right\}\end{aligned} \tag{23}$$

The obtained values of c_1 to c_5 are 0.86, 0.54, 0.90, -0.67, and -0.56. Comparisons between Equations (22) and (19) and between Equations (23) and (20) show that Equations (22) and (23) represent the velocity skewness and atiltness in the field well (**Figure 3**).

4.5 Beach profile change

Change in the beach profile is estimated on the basis of a continuity equation (Equation (24)) and the cross-shore gradient of the cross-shore sediment transport rate. The alongshore gradient of the longshore sediment transport rate is assumed to be negligible.

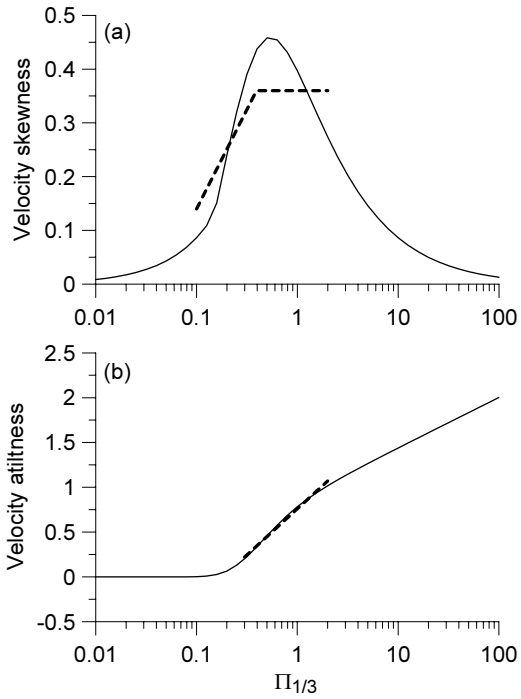

Figure 3 (a) Relationship between velocity skewness and $\Pi_{1/3}$. The solid and broken lines represent Equations (22) and (19), respectively. (b) Relationship between velocity atiltness and $\Pi_{1/3}$. The solid and broken lines represent Equations (23) and (20), respectively.

$$\frac{\Delta z}{\Delta t} = -\frac{1}{1-\lambda}\frac{\Delta Q}{\Delta x} \tag{24}$$

where z is the elevation, which is positive in the upward direction, t is the time, λ is the porosity (= 0.3), and Q is the cross-shore sediment transport rate, which is positive in the seaward direction, per unit length in the alongshore direction.

The cross-shore sediment transport rate is assumed to be made up of four contributions due to sediment suspension and undertow Q_s, near-bottom velocity skewness and amplitude $Q_{b,v}$, near-bottom acceleration skewness $Q_{b,a}$ and beach slope $Q_{b,slope}$.

The value of Q_s is expressed in Equation (25) on the basis of the assumption that the amount of suspended sediments is proportional to the surface roller energy dissipation rate, as assumed by Kobayashi et al. (2008).

$$Q_s = \alpha_1\frac{D_r}{\rho g(s-1)w_f}U \tag{25}$$

where α_1 is a coefficient, s is the sediment specific gravity

and w_f is the sediment fall velocity.

The spatial distribution of suspended sediment transport rate in the field is expected to be smoother than that of Q_s as estimated by Equation (25) due to the effects of advection and diffusion of suspended sediment, which are not included in the present model. Thus, the spatial distribution of Q_s as estimated by Equation (25) is smoothed by the triangular filter expressed by Equation (26). The smoothing number was determined in the calibration described below.

$$Q_{s,i,m} = \left(Q_{s,i-1,m-1} + 2Q_{s,i,m-1} + Q_{s,i+1,m-1}\right)/4 \quad (26)$$

where i is the grid number and m is the smoothing number.

On the basis of Bailard's (1981) formula, the value of $Q_{b,v}$ is assumed to be

$$Q_{b,v} = -\alpha_2((\sqrt{\beta_1})_u u_{b,rms}^3 \cos\theta + (u_{b,rms}^2 + u_{bl,rms}^2)V \sin\theta\cos\theta) \quad (27)$$

where α_2 is a coefficient (s^2/m) and $u_{bl,rms}$ is the amplitude of long-period near-bottom velocity, which is estimated on the basis of Goda (1975) using Equation (28).

$$u_{bl,rms} = 0.01\sqrt{g/h}\left[1/\sqrt{(H_0/L_0)(1+h/H_0)}\right]H_0 \quad (28)$$

Bailard's (1981) formula includes terms related to the near-bottom time-averaged velocity. The near-bottom time-averaged velocity in the surf zone is seaward and relatively large, but its accurate prediction is still a great challenge, despite several methods having been proposed (e.g., Garcez-Faria et al., 2000; Reniers et al., 2004). Hence, in this study, $Q_{b,v}$ is assumed not to include a term for sediment transport rate due to the near-bottom time-averaged velocity, which may be counted in Q_s.

The value of $Q_{b,a}$ is expressed by Equation (29), as given by Hoefel and Elgar (2003).

$$Q_{b,a} = -\alpha_3\left((\beta_3)_u a_{b,rms} - a_{cr}\left|(\beta_3)_u\right|/(\beta_3)_u\right)\cos\theta, \quad \left|(\beta_3)_u a_{b,rms}\right| > a_{cr} \quad (29)$$

$$Q_{b,a} = 0, \quad \left|(\beta_3)_u a_{b,rms}\right| \le a_{cr}$$

where α_3 is a coefficient (m s), $a_{r,rms}$ is the amplitude of near-bottom acceleration and a_{cr} is a threshold value (= 0.2 m/s^2).

The value of $Q_{b,slope}$ is also based on that of Bailard (1981).

$$Q_{b,slope} = \alpha_4 \frac{\tan\beta}{\tan\phi}\left(u_{b,rms}^3 + u_{bl,rms}^3\right) \quad (30)$$

where α_4 is a coefficient (s^2/m) and ϕ is the internal friction angle of the sediment (= 30 degrees). Although Bailard (1981) assumed α_4 was equal to α_2, α_4 in this study is assumed to be different from α_2.

5. Calibration

The parameters α_1 to α_4 included in the equations representing the four types of cross-shore sediment transport rates and the smoothing number for the suspended load were determined from beach profile data obtained at HORS between January and December 1989.

5.1 Model setup

The cross-shore grid size was set at 5 m, and the time interval was 2 hours. The seaward boundary was set at P1200m, where the elevation was -10.7 m based on the Hasaki datum level. The input data at the seaward boundary were the wave heights and periods estimated from values measured with the wave gage at a water depth of about 24 m (see location on **Figure 1**), the wave angles estimated by Hashimoto et al. (2000) using WAM, a third generation wave prediction model, and the estimated astronomical tide levels.

The initial beach profile shoreward of P385m was set as the profile measured on January 4, 1989, and that seaward of P445m was set as the mean beach profile shown in **Figure 2**. The profile between P390m and P440m was interpolated from the elevations at P385m and P445m.

The values of C_{br} and C_B in Equations (1) and (3) were set to 0.70 and 0.75, respectively, so that the error between the significant wave heights measured (Kuriyama et al., 2008b) and predicted along the HORS pier during the period from 1987 to 2001 was minimal. The values of ν in Equation (14) and k_a in Equation (16) were set at 5.0 m^2/s and 0.15 m as used by *Kuriyama* (2010b) for HORS long-term longshore current velocity data.

The parameters in the cross-shore sediment transport rate formulae (Equations (25), (27) and (29)) and the smoothing number for the suspended load were determined so that the error function described below was minimal using SCE-UA algorism (Shuffled Complex Evolution – University of Arizona) (Duan et al., 1993) as in the study of Ruessink et al. (2007). The error function F in the calibration was set as the sum of the relative errors in elevation and bar crest position, which are represented by the first and second terms of the right-hand side of Equation (31).

$$F = \frac{\sum_{x,t}\left(z_p(x,t) - z_m(x,t)\right)^2}{\sum_{x,t}\left(z_m(x,t) - z_m(x,0)\right)^2} + \frac{\sum_{t}\left(x_{c,p}(t) - x_{c,m}(t)\right)^2}{\sum_{t}\left(x_{c,m}(t) - 180\right)^2} \quad (31)$$

where x_c is the bar crest position and the subscripts p and m denote the predicted and measured values, respectively. The locations of the bar crest and trough were defined as the points where the beach slope changes, looking offshore, from a negative value to a positive value and vice versa. A bar was defined in this study as one with a bar height (the difference between the elevations at the crest and the shoreward trough) larger than 0.5 m. The baseline prediction for the relative error in elevation is the initial beach profile and that in bar crest position is P180m, where most bars at Hasaki were generated and started to migrate seaward. The second term of Equation (31) is calculated when a bar is observed in the measurement. The second term was added into the error function because there is a possibility that the first term cannot precisely evaluate the model performance in the bar migration direction as suggested by van Rijn (2003).

5.2 Calibration result

The optimal parameters obtained were α_1 = 1.147 x 10^{-3}, α_2 = 7.651 x 10^{-4} (s^2/m), α_3 = 9.96 x 10^{-5} (m s) and α_4 = 7.755 x 10^{-4} (s^2/m), and the smoothing number was 15. The relative errors in elevation and bar crest position, represented by the first and second terms of the right-hand side of Equation (31), were 0.609 and 0.093, respectively.

The model closely predicted the bar crest positions for almost 2 years including the 1-year calibration period of 1989 and the following year of 1990 (**Figures 4 and 5**); the input offshore significant wave height and period are shown in **Figure 6**. The seaward bar migration from January 1989 and the generation of a new bar at P200m at the end of 1989 were well predicted in the model. Even in 1990, after the calibration period, although the predicted bar crest location was slightly shoreward of the measured one, the model successfully predicted the seaward bar migration between January and April and the shoreward migration between April and September.

The model also performed well with respect to the changes in the beach profile (**Figure 7**). The predicted bar crest location and elevation agreed well with field measurements taken in 1989, although the model performed less well in the

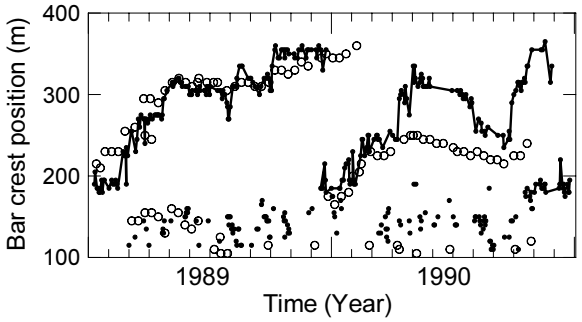

Figure 4 Time series of measured (solid circles) and predicted (open circles) bar crest positions. The solid lines show the series of bar migrations.

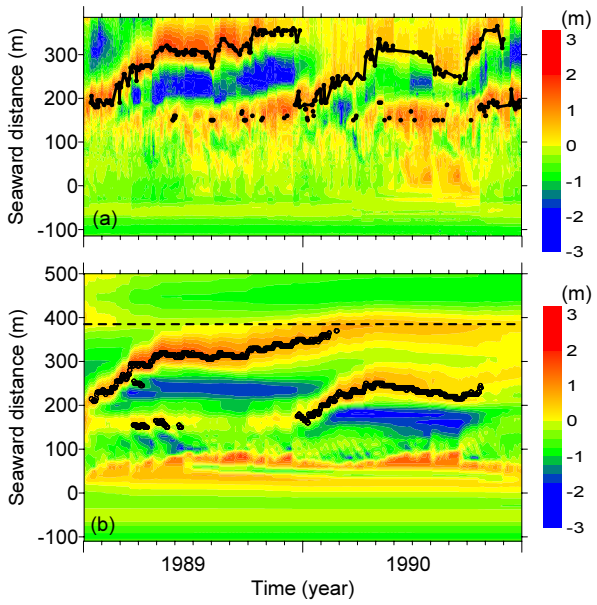

Figure 5 Spatial and temporal variations of measured (a) and predicted (b) elevations on the basis of the mean beach profile (**Figure 2**). Elevations above and below the mean beach profile are indicated by warm and cold colors, respectively. The horizontal broken line in (b) shows the location of the tip of the pier. See **Figure 5** for further explanation.

foreshore than in the bar-trough zone. In 1990, the predicted location of the bar crest was shoreward of the measured one as mentioned above, which resulted in an increase in the discrepancy between the prediction and measurement. After November 1990, the predicted profile became flat and the bar was not prominent.

The model performance mentioned above is reflected in the Brier skill score *BSS* (Murphy and Epstein, 1989), defined by Equation (32). The value of *BSS* is equal to 1 when the

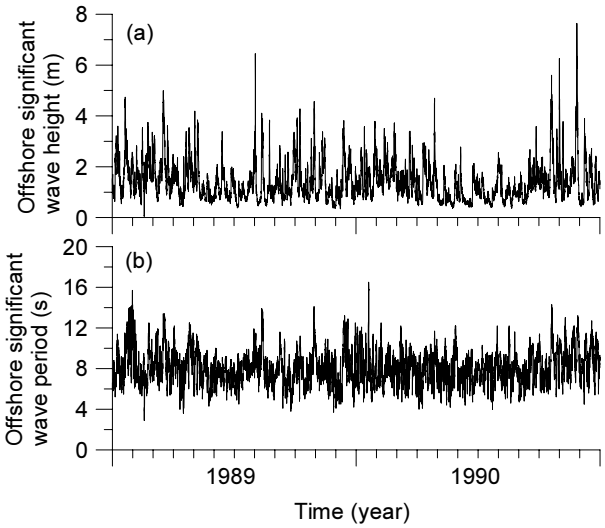

Figure 6 Input offshore significant wave height (a) and period (b) during the period from 1989 to 1990.

prediction perfectly matches the measurement and falls below 0 when the model performance is poorer than the model that assumes no change.

$$BSS = 1 - \frac{\sum_{x,t}\left(z_p(x,t) - z_m(x,t)\right)^2}{\sum_{x,t}\left(z_m(x,t) - z_m(x,0)\right)^2} \qquad (32)$$

The *BSS* value was above 0 in the region between P-65m and P355m, which includes the foreshore, inner surf zone and bar-trough zone, by the middle of December 1990, and over 0.5 in the bar-trough region (P205m to P535m) at the end of 1990 (**Figure 8**). This result indicates that the model well reproduced the cyclic bar migrations for an interval of about 2 years including the 1-year calibration period.

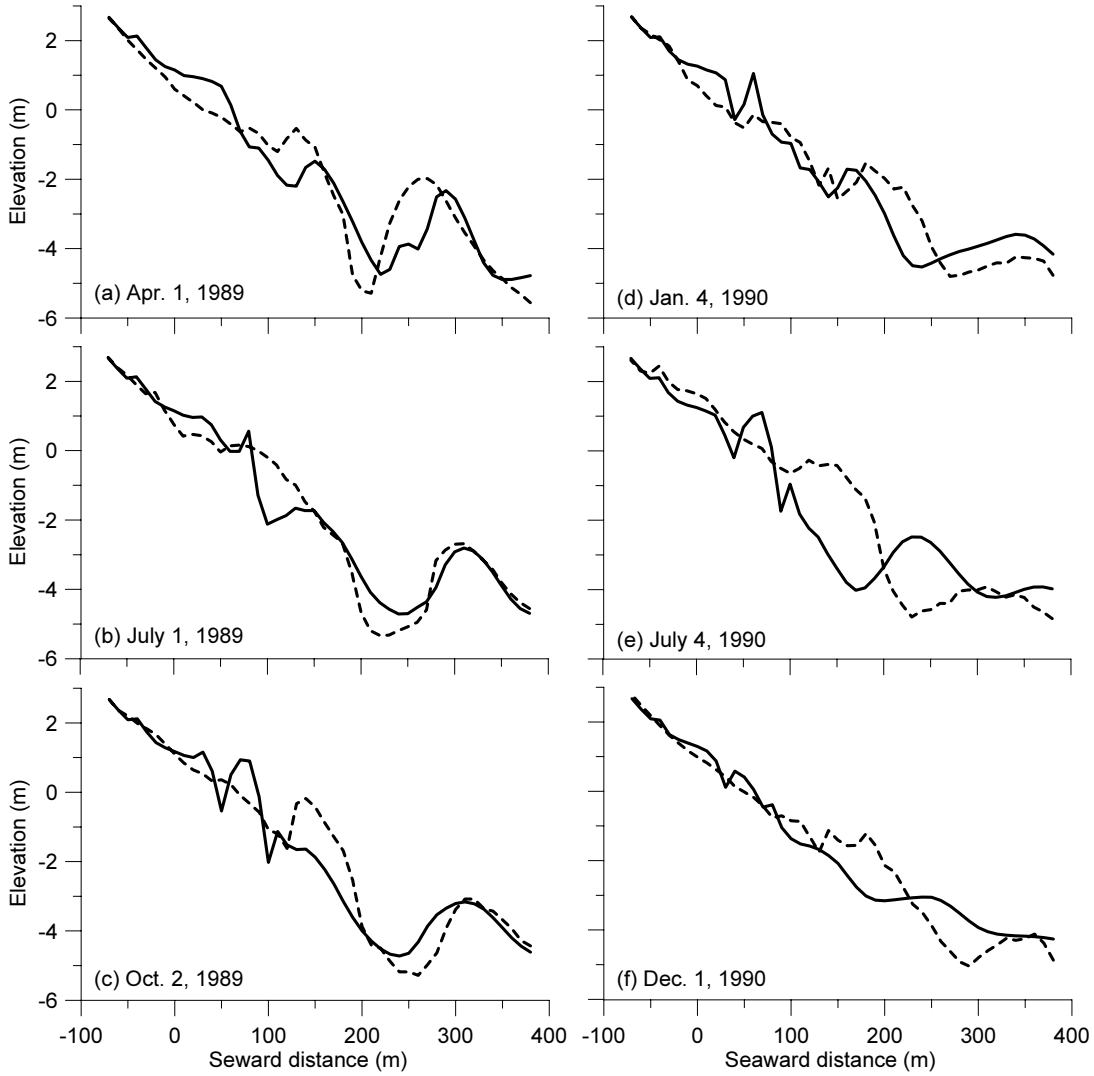

Figure 7 Measured (broken lines) and predicted (solid lines) beach profiles. (The broken lines show the initial beach profile on January 4, 1989.)

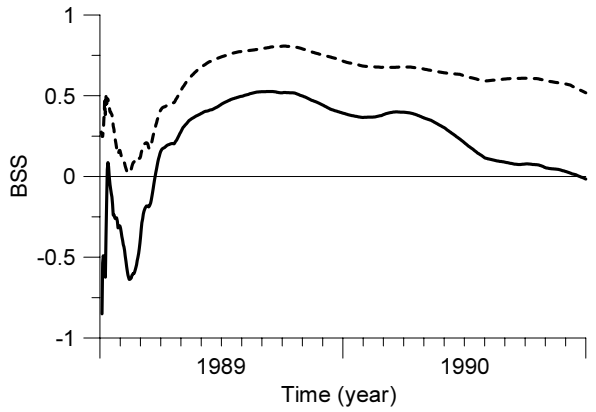

Figure 8 Time series of the model skill score *BSS* in the region from P-65 m to P355 m (solid line) and that from P205m to P355m, the bar-trough region (broken line).

6. Application for bar migrations from 1991 to 2000

The model performance outside the calibration period was examined by comparing the beach profile data obtained during a 10-year period from January 1991 to December 2000. The period was divided into five 2-year blocks. The input offshore significant wave heights and periods during this interval are shown in **Figure 9**.

The *BSS* value in the bar-trough zone was higher than that in the whole region (**Figure 10**) as was the case for the calibration period, and the *BSS* value in the bar-trough region was above 0 at the end of the calculations for three of the five blocks.

During the period from 1991 to 1992, the prediction successfully reproduced the seaward bar migration occurring from January 1991 and a new bar formation at around P190m in October 1991 as well as its subsequent seaward migration (**Figures 11 (a), 12 (a) and 12 (f)**). However, the bars and troughs were more developed in the prediction than in the measurement, which resulted in *BSS* values below 0 in the bar-trough region from October 1991 (**Figure 10**).

The model also reproduced the seaward bar migration from January 1993 and a new bar formation at around P185m in April 1993 (**Figures 11 (b), 12 (b) and 12 (g)**). Subsequently, however, the bar in the model prediction decayed and the bar height fell to lower than 0.5 m, which was not compatible with the field observations.

As shown in **Figures 11 (c), 12 (c) and 12 (h)**, although the seaward bar migration from January 1995 was reproduced in

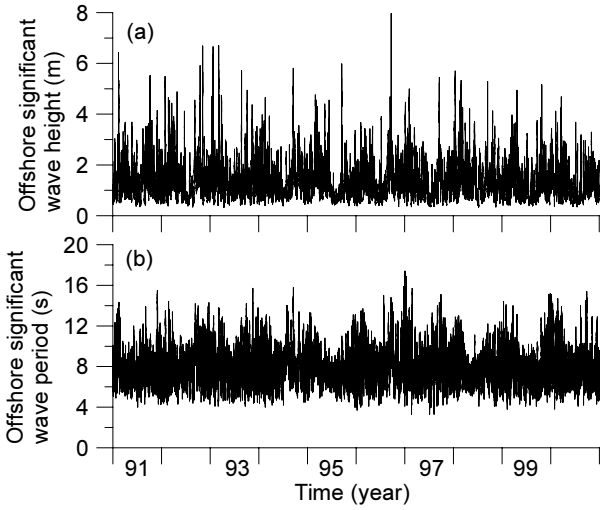

Figure 9 Input offshore significant wave height (a) and period (b) during the period from 1991 to 2000.

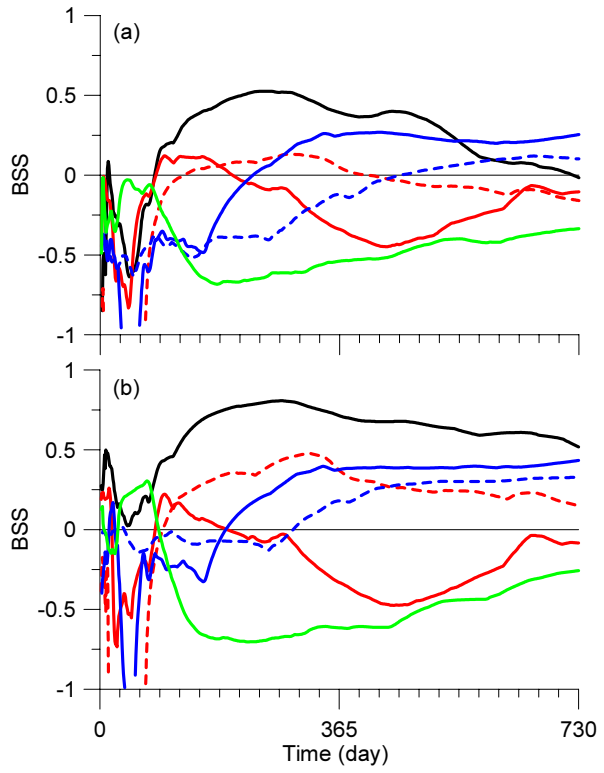

Figure 10 Time series of *BSS* for the regions from P-65m to P355m (a) and from P205m to P355m (bar-trough zone) (b). The black, solid red, broken red, solid blue, broken blue and green lines show the values during the periods from 1991 to 1992, from 1993 to 1994, from 1995 to 1996, from 1997 to 1998, and from 1999 to 2000.

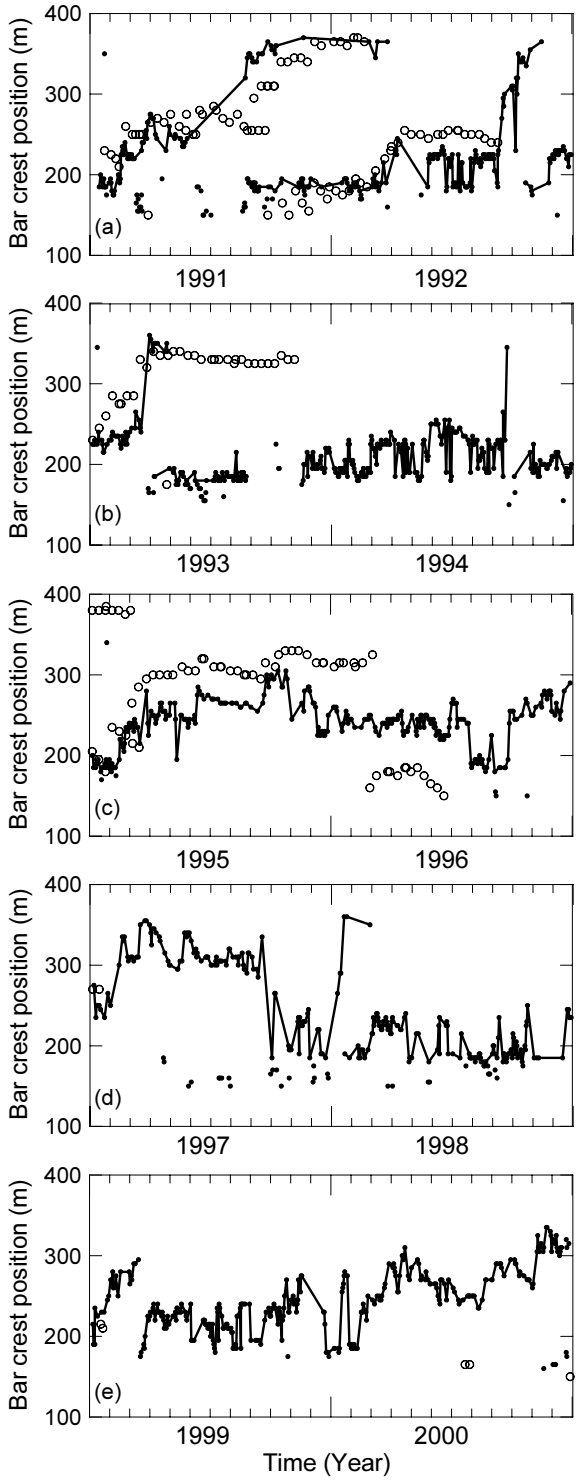

Figure 11 Bar crest positions measured and predicted during the periods from 1991 to 1992 (a), from 1993 to 1994 (b), from 1995 to 1996 (c), from 1997 to 1998 (d), and from 1999 to 2000 (e). See **Figure 4** for further explanation.

the model prediction, the migration rate was faster in the prediction than that in the measurement and the location of the bar in the model prediction was seaward of that in the measurement.

During the period from 1997 to 1998, the model predicted a flatter beach profile than that which was measured (**Figures 12 (d) and (i)**) and did not predict the formation of bars, which are defined here as those with heights greater than 0.5 m (**Figure 11 (d)**). However, at around P320m during the period from January to September 1997 and at around P200m during the period from October to December 1997, where and when bars were formed in the measurement, the model predicted elevations higher than the mean beach profile (**Figures 12 (d) and (i)**).

The *BSS* value was much lower during the 1999-2000 interval, both in the bar-trough region and the whole region, than in the other intervals (**Figure 10**). The reason for this is that the model could not reproduce the changes in the beach profile including seaward bar migration and new bar formation between March 15 and 25 in 1999 (**Figures 11 (d), 12 (d) and 12 (j)**), during which time two storms with wave heights exceeding 3.0 m attacked the beach although such wave heights during a storm were not unusually large. The reason for this discrepancy between the predicted and measured profiles is still unclear.

As mentioned above, even when the predicted profile does not technically contain a bar because the bar height is smaller than 0.5 m, an area above the mean beach profile is sometimes formed in the model prediction at around the bar crest position in the measurement. In this case, it appears that the model is capable of predicting bar migrations not quantitatively but qualitatively. Hence, the centers of areas that are 0.2 m higher than the mean beach profile and have cross-shore lengths longer than 20 m were compared in the prediction and measurement.

Except for the period from 1999 to 2000, the centers of the accumulation areas in the prediction and measurement agree well (**Figure 13**) and the Brier skill scores for the centers of accumulation areas BSS_c, defined by Equation (33), are mostly above 0 (**Figure 14**). This result indicates that the model in this study predicted cyclic bar evolutions during an 8-year period from 1991 to 1998 (i.e., outside the calibration period) at least qualitatively.

$$BSS_C = 1 - \frac{\sum_t \left(X_{c,p}(t) - X_{c,m}(t)\right)^2}{\sum_t \left(X_{c,m}(t) - X_{c,m}(0)\right)^2} \tag{33}$$

where X_c is the center of an area above the mean beach profile.

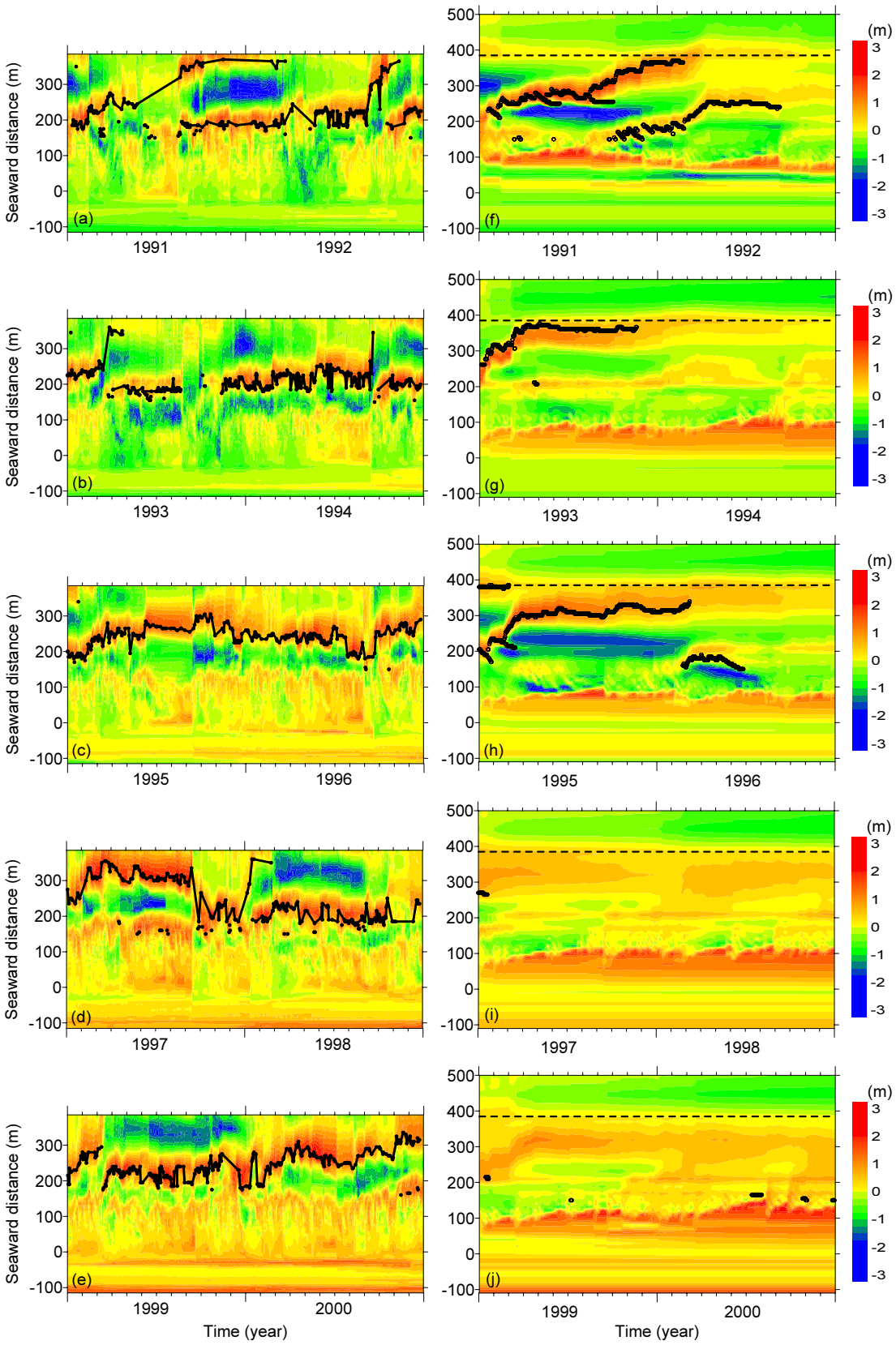

Figure 12 Spatial and temporal variations of the measured ((a) to (e)) and predicted ((f) to (j)) elevations on the basis of the mean beach profile (**Figure 2**) during the periods from 1991 to 1992 (a, f), from 1993 to 1994 (b, g), from 1995 to 1996 (c, h), from 1997 to 1998 (d, i), and from 1999 to 2000 (e, j). See **Figure 5** for further explanation.

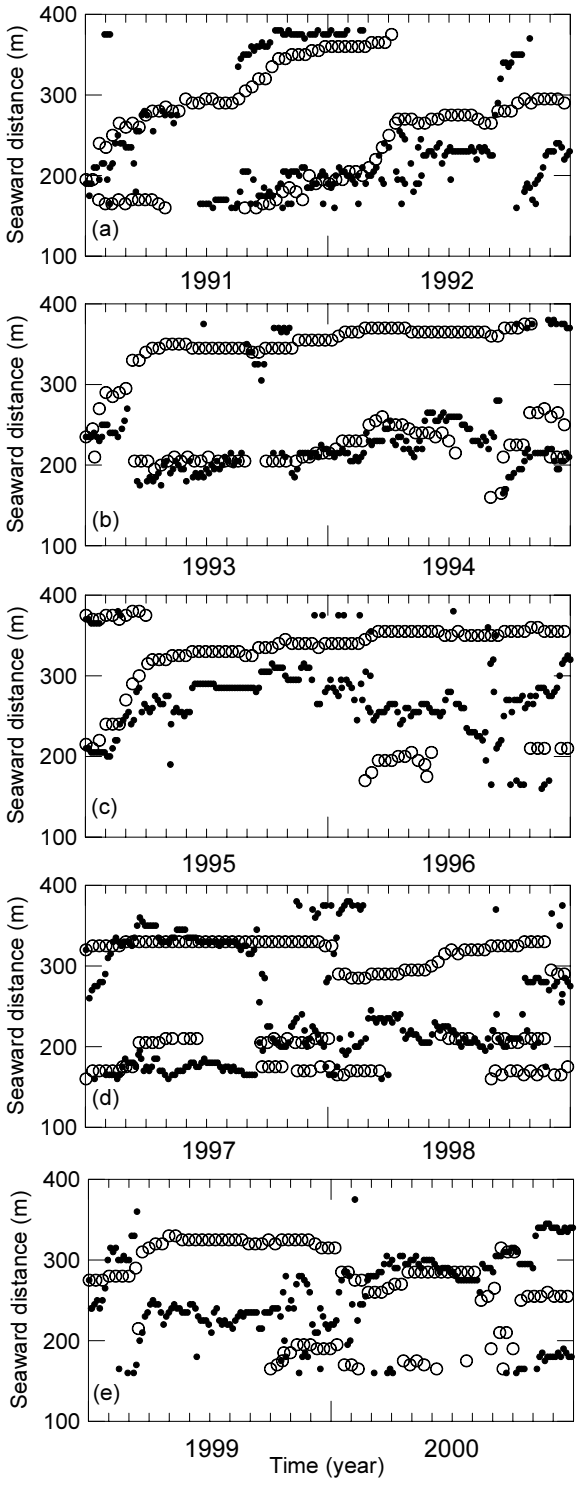

Figure 13 Measured (solid circles) and predicted (open circles) centers of areas above the mean beach profile during the periods from 1991 to 1992 (a), from 1993 to 1994 (b), from 1995 to 1996 (c), from 1997 to 1998 (d), and from 1999 to 2000 (e).

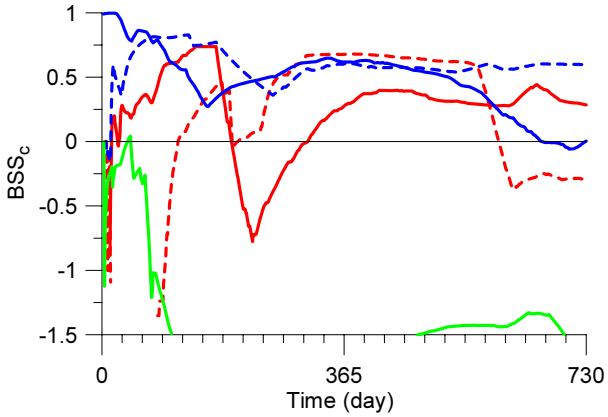

Figure 14 Time series of BSSc. The black, solid red, broken red, solid blue, broken blue and green lines show the values during the periods from 1991 to 1992, from 1993 to 1994, from 1995 to 1996, from 1997 to 1998, and from 1999 to 2000.

7. Discussion

7.1 Sediment transport rate

The seaward suspended transport rate Q_s was relatively large at the bar crest and shoreward of P150m (**Figure 15**). In particular, it was large when the bar migrated seaward, which would suggest that the seaward suspended load made a major contribution to the seaward migration of the bar.

The shoreward bed load $Q_{b,v}$, mainly induced by near-bottom velocity skewness, was also large at the bar crest and shoreward of P150m as with the suspended load, whereas the shoreward bed load induced by near-bottom acceleration skewness $Q_{b,a}$ was large near the shoreline. The bed load due to the beach slope $Q_{b,slope}$ was smaller than the three transport rates mentioned above.

7.2 Sensitivities of calibration results to calibration period and error function

(1) Calibration period

To investigate the influence of the calibration period on the results, the model was calibrated with 6-month and 2-year data sets starting from January 4, 1989. The smoothing number was fixed to be 15 and the obtained parameter values were $\alpha_1 = 1.123 \times 10^{-3}$, $\alpha_2 = 9.405 \times 10^{-4}$ (s^2/m), $\alpha_3 = 1.099 \times 10^{-4}$ (m s) and $\alpha_4 = 9.239 \times 10^{-4}$ (s^2/m) for the 6-month calibration period and $\alpha_1 = 1.144 \times 10^{-3}$, $\alpha_2 = 8.595 \times 10^{-4}$ (s^2/m), $\alpha_3 = 7.96 \times 10^{-5}$ (m s) and $\alpha_4 = 7.925 \times 10^{-4}$ (s^2/m) for the 2-year period.

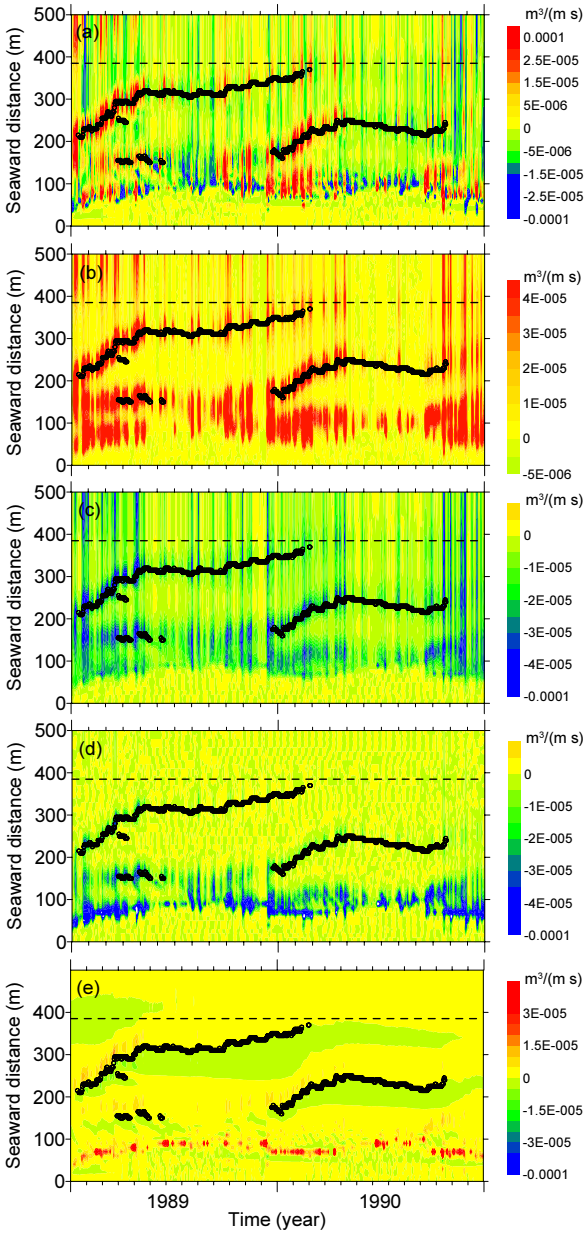

Figure 15 Spatial and temporal variations of the predicted cross-shore sediment transport rate Q (a), suspended sediment transport rate Q_s (b), bed transport rate due to near-bottom velocity skewness and amplitude $Q_{b,v}$ (c), bed transport rate due to near-bottom acceleration skewness $Q_{b,a}$ (d) and bed transport rate due to beach slope $Q_{b,slope}$ (e). Positive values, shown by warm colors, represent seaward transport rates.

In the case of the 6-month calibration period, the predicted profiles were flattened more quickly than the profiles calibrated with the 1-year calibration period used in this study, and in May 1990, the bar predicted in the model was shown to decay (**Figure 16**). In the case of the 2-year calibration period, on the other hand, although *BSS* values in the region between

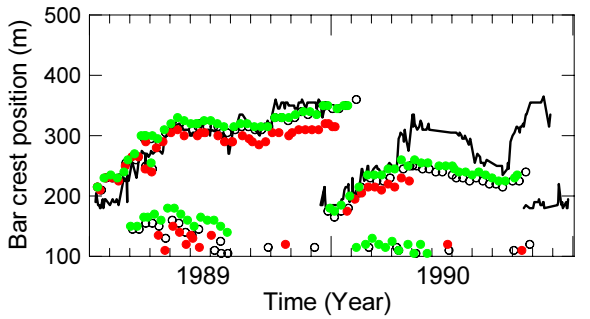

Figure 16 Time series of bar crest positions predicted with 6-month (red solid circles) and 2-year (green solid circles) calibration periods. See **Figure 4** for further explanation.

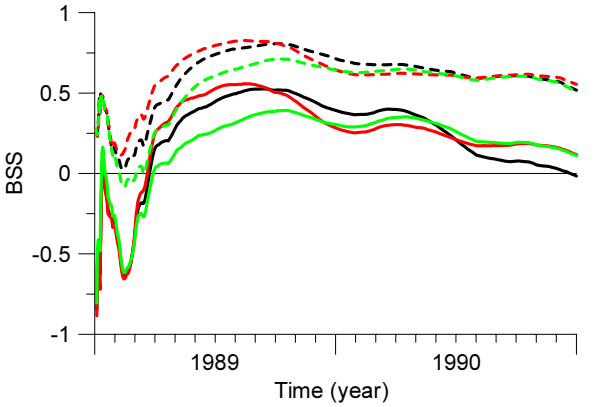

Figure 17 Time series of the model skill score *BSS* for 6-month (red lines) and 2-year (green lines) calibration periods. See **Figure 8** for further explanation.

P-65m and P355m were lower in 1989 and higher in 1990 than those in the 1-year calibration period (**Figure 17**), the bar crest positions predicted with the 2-year and 1-year calibration periods agree well (**Figure 16**). These results suggest that the model used in the combination with the 6-month calibration period cannot predict the cyclic bar migrations quantitatively, but the model used in conjunction with the 2-year calibration period is successful in doing so. In order to reproduce cyclic bar migrations, a calibration period covering at least one bar migration cycle, composed of bar formation, development and decay, is recommended.

(2) Error function

To investigate the influence of the error function, which was defined by Equation (31) as the sum of the errors in elevation and bar crest position, the calibration results with two error functions were compared. One error function was composed only of the relative error in elevation, whereas in

the second error function the weight of the relative error in bar crest position was doubled. The smoothing number was fixed to be 15. The obtained parameter values for the former error function were α_1 = 1.159 x 10^{-3}, α_2 = 7.27 x 10^{-4} (s^2/m), α_3 = 9.94 x 10^{-5} (m s) and α_4 = 8.189 x 10^{-4} (s^2/m), whereas those for the latter error function were the same as those obtained through the standard calibration procedure as shown in **4.2**.

Although the decay of the bar as predicted with the parameter set for the former error function is slightly earlier than that for the error function defined by Equation (31), both bar crest positions agree well with the observations (**Figure 18**). The *BSS* value for the former error function is close to that for the error function defined by Equation (31) (**Figure 19**). These results, as well as the fact that the parameter values obtained with the latter error function are the same as those obtained through the standard calibration procedure, indicate that the calibration result in this study was not strongly sensitive to the error function.

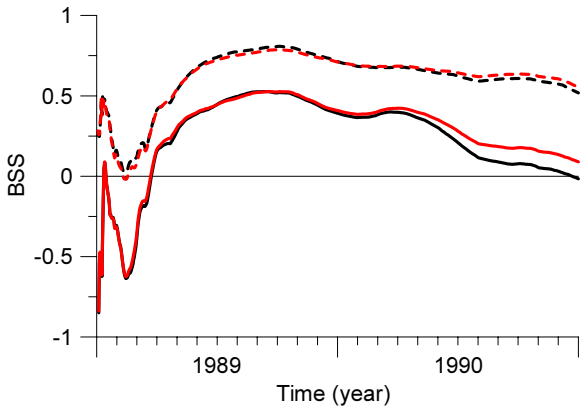

Figure 18 Time series of the model skill score *BSS* for error function composed only of relative error in elevation (red lines). See **Figure 8** for further explanation.

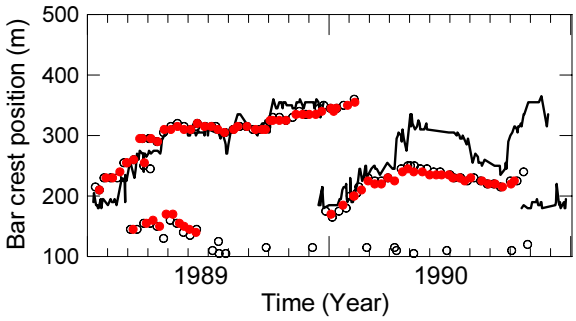

Figure 19 Time series of bar crest positions calibrated with error function composed only of relative error in elevation (red solid circles). See **Figure 4** for further explanation.

7.3 Sensitivities of prediction results to parameter values and initial beach profile

(1) Parameter values

Sensitivity tests were conducted by changing the α_1 to α_4 parameter values by 10% in the model predictions. The parameter to which the modeling results were most sensitive was the value of α_1 for suspended load. The bar predicted in the model migrated more quickly with a 10% increase in α_1 and more slowly with a 10% decrease, and the differences between the bar crest positions predicted with the altered α_1 and those predicted with the optimal α_1 at the end of the calibration period (December 1989) were approximately 50 m (**Figure 20**). The parameter to which the results showed second greatest sensitivity was the value of α_4 for bed load due to beach slope; the differences in the bar crest position with the altered parameter values were 25 m (**Figure 21**). Parameters α_2 and α_3 for bed load due to velocity and acceleration skewness, respectively, exerted the least influence on the model predictions.

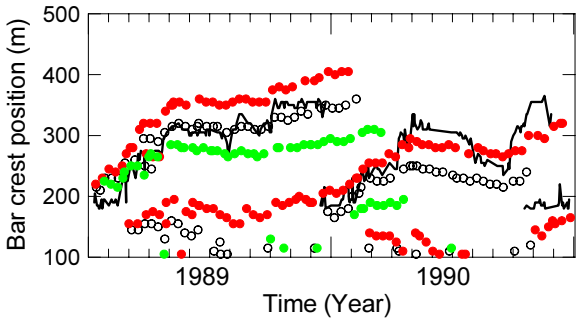

Figure 20 Bar crest positions with α_1 increased (red circles) and decreased (green circles) by 10 %. See **Figure 4** for further explanation.

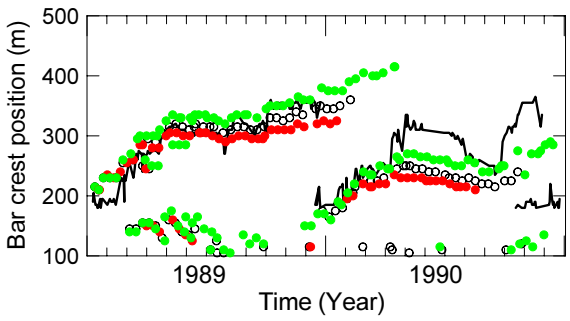

Figure 21 Bar crest positions with α_4 increased (red circles) and decreased (green circles) by 10 %. See **Figure 4** for further explanation.

(2) Initial beach profile

To examine whether the model's predictions of beach profile are dependent on the initial condition, as in deterministic chaos, the beach profile measured on January 5 and 6, 1989, were used as the initial profiles in the predictions (**Figure 22**). The standard deviations of the elevation differences from the profile on January 4 (the initial profile in the calibration) in the region between P-65m and P355m for profiles on January 5 and 6 were 0.12 m and 0.15 m, respectively. The result is that, although there are small discrepancies between foreshore profiles when using different initial profiles, the small differences in the initial profiles did not lead to a large difference in the prediction results (**Figure 23**). This conclusion is consistent with that of Ruessink and Kuriyama (2008).

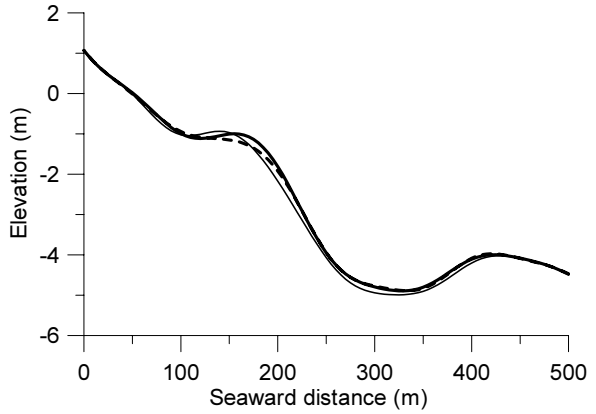

Figure 22 Beach profiles on January 4 (thin solid lien), 5 (thick solid line) and 6 (broken line).

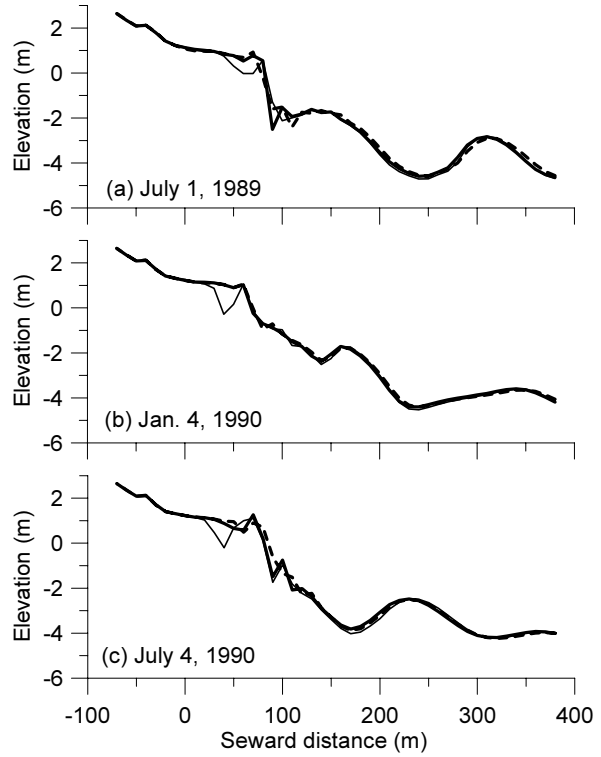

Figure 23 Beach profiles predicted with initial profiles on January 4 (thin solid lien), 5 (thick solid line) and 6 (broken line).

7.4 Smoothing of suspended sediment transport rate

The effect of smoothing suspended load was investigated by comparing the smoothed suspended sediment concentrations and those computed using an advection-diffusion equation of the depth-averaged suspended sediment concentration.

$$\frac{\partial (hC)}{\partial t} = \frac{\partial (hCU)}{\partial x} + \frac{\partial}{\partial x}\left(\nu_H \frac{\partial (hC)}{\partial x} \right) + \frac{\alpha_1 D_r}{\rho g (s-1) w_f} W - C w_f \tag{33}$$

where ν_H is the horizontal diffusion coefficient set to 0.1 m^2/s as by Grunnet et al. (2004). The velocity of sediment suspension W is different from the sediment fall velocity w_f in ordinary advection and diffusion calculations. However, in this study, the suspended sediment concentration was assumed to be proportional to the surface roller energy dissipation rate, and hence the computation of the suspended sediment concentration was conducted by assuming W was equal to w_f.

In the computation, two representative profiles at Hasaki were used. The first was the profile measured on February 2, 1989, which included a bar crest at P185m and the second was that measured on June 2, 1989, with a crest at P310m. The input offshore significant wave heights were 1.0, 2.0 and 3.0 m and the wave period was 8.0 s. The sediment diameter was assumed to be 0.2 mm. The suspended sediment concentration value after smoothing was obtained by dividing the smoothed suspended sediment transport rate by the undertow velocity.

The peak values of smoothed suspended sediment concentration were about 1.3 to 1.7 times those computed with advection and diffusion and were located shoreward of the locations of peak in the advection and diffusion computation (**Figure 24**). However, to some extent, the smoothing of the suspended load incorporated the effects of

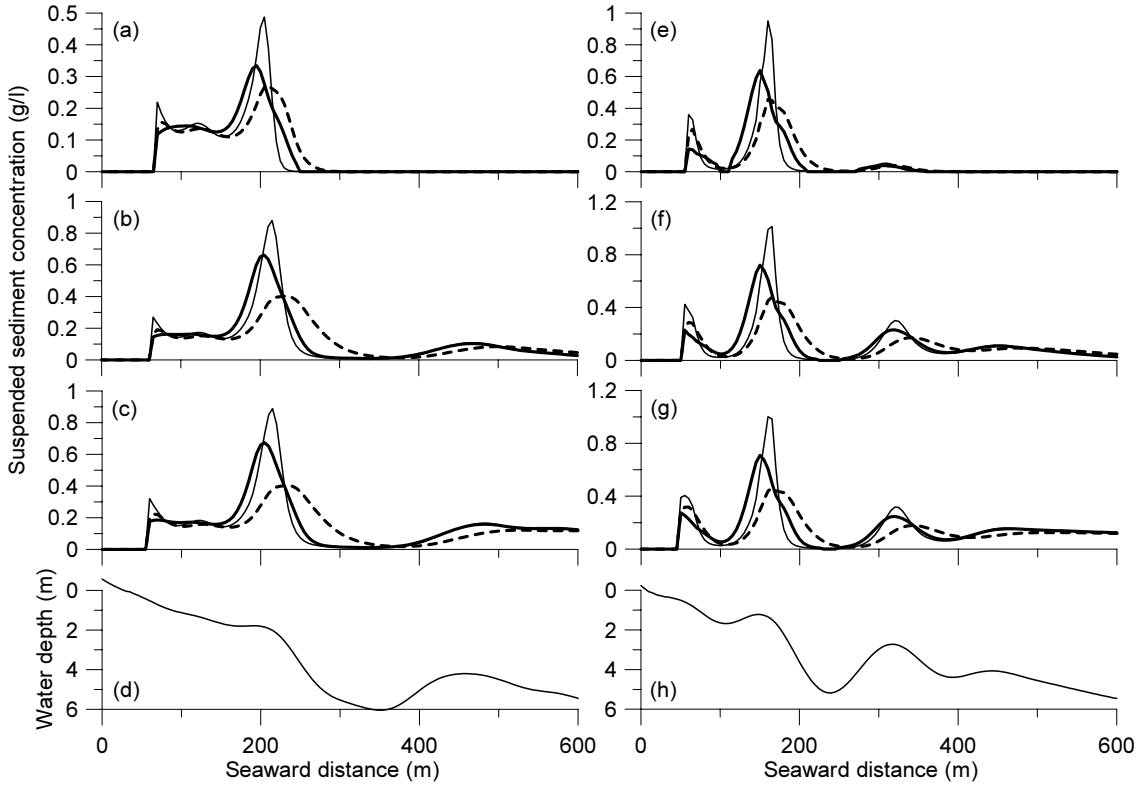

Figure 24 Comparisons among suspended sediment concentrations before (thin solid lines) and after (thick solid lines) the smoothing and computed by the advection-diffusion equation (broken lines). Panels (a) to (c) show the values for the profile (d), and panels (e) to (g) for the profile (h). The deepwater wave heights are 1 m ((a, e)), 2 m ((b, f)) and 3 m ((c, g)).

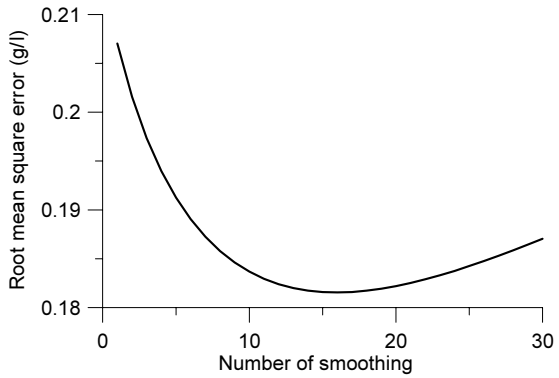

Figure 25 Root-mean-square error in suspended sediment concentration versus number of smoothing.

advection and diffusion of the suspended sediment concentration into the model. Furthermore, the root-mean-square error between the smoothed and computed suspended sediment concentrations in the region between P100m and P550m was minimal with a smoothing number of 16 (**Figure 25**), which is close to the smoothing number obtained in the calibration, 15.

7.5 Parameter values

The optimal parameter values were found to be α_1 = 1.147 x 10^{-3}, α_2 = 7.651 x 10^{-4} (s^2/m), α_3 = 9.96 x 10^{-5} (m s) and α_4 = 7.755 x 10^{-4} (s^2/m), as mentioned in section **5.2**. The value of α_1, for the suspended load, is about twice Kobayashi et al.'s (2008) value of 5.0 x 10^{-4}. However, as shown above, the smoothing of the suspended load reduces the peak values, and thus the suspended transport rate estimated by the present model would be 1.5-2 times the value of Kobayashi et al. (2008).

For the bed load, α_2 is approximately half the value of 4.09 x 10^{-4} (s^2/m) used by Gallagher et al. (1998) and almost the same as the value of 6.27 x 10^{-4} (s^2/m) used by Hsu et al. (2006), while α_3 is about two-thirds the value of 1.4 x 10^{-4} (m s) used by Hoefel and Elgar (2003). Although there are some discrepancies between the optimal parameter values in this study and those used in previous studies, they are in reasonable agreement.

The value for α_4 was assumed to be different from α_2 in the calibration, while both were given the same value in the study

of Bailard (1981). The optimal α_4 value of 7.755 x 10^{-4} (s^2/m) is almost the same as the optimal α_2 value of 7.651 x 10^{-4} (s^2/m).

These results along with those regarding the smoothing number in section **7.4** support the idea that the calibration was reasonably conducted.

7.6 Model performance outside calibration period

Pape et al. (2009) applied data-driven models using a neural network and a process-based model to bar migrations at Hasaki. They divided the period from 1987 to 2000 into 16 blocks, each including a series of bar migrations, and predicted the bar migrations during each of the 16 blocks. Even with parameter sets optimal for each block, the performance of the model was highly variable over the 16 blocks including some blocks with very poor results. They therefore concluded that model prediction of bar migration at Hasaki was difficult.

The results of this study during the period from 1991 to 2000 (i.e., outside the period used for calibration) also show that the model skill score for the elevation *BSS*, as defined by Equation (30), was high during some periods, although *BSS* values were not necessarily high overall (**Figure 10**). Interestingly, however, measured cyclic seaward bar migrations are represented in the modeling results by the migrations of accumulation areas, which are higher than the mean beach profile. Hence, it is concluded that the model used in this study can reproduce the cycles of seaward bar evolution at Hasaki at least qualitatively.

8. Conclusions

A process-based one-dimensional model for beach profile change was developed to predict cyclic bar evolutions. The model estimated beach profile change on the basis of the cross-shore gradient of the cross-shore sediment transport rate, which was assumed here to be made up of the suspended transport rate due to wave breaking and the bed transport rates due to near-bottom velocity and acceleration and beach slope.

The model was calibrated with beach profile data obtained every weekday at 5-m intervals along a 400-m-long pier at the Hazaki Oceanographical Research Station (HORS), located on the Hasaki coast of Japan, during a 1-year period from January to December 1989. In the computation, the grid size was set at 5 m and the time interval was 2 hours. The optimal values of the parameters included in the cross-shore sediment transport rate formula and the smoothing number of suspended load were obtained so that the error function denoting the sum of the relative errors in elevation and bar crest position was minimal.

The bar migrations over a period of 2 years including the 1-year calibration period of 1989 and the following year of 1990 were predicted by the model using the optimal parameter set and the optimal smoothing number. The predicted bar crest positions agreed well with those measured in the field, and the Brier skill score for elevation was above 0 by the middle of December 1990 shoreward of the tip of the pier including the foreshore, inner surf zone and bar-trough zone and over 0.5 in the bar-trough zone at the end of 1990. These results indicate that the model quantitatively predicted the cyclic bar migrations from 1989 to 1990.

The obtained optimal parameter values are 0.5 to 2 times the values used in previous studies, and hence they are thought to be in good agreement. The smoothing number of the suspended sediment transport rate was also confirmed to be effective in incorporating the influences of the advection and diffusion of suspended sediment into the model.

The model was applied to bar migrations outside the calibration period, during a 10-year period from 1991 to 2000, which was divided to five 2-year blocks. The Brier skill scores for elevation were not necessarily high for all blocks, but most of the bar crest movements detected by field measurements were expressed in the model by the movements of the areas above the mean beach profile, and the Brier skill scores for the center of the area above the mean beach profile were high for all blocks except for the 1999-2000 period. Hence, it is concluded that the model used in this study can predict cyclic bar evolutions at Hasaki even outside the calibration period at least qualitatively.

(*Received on January 25, 2010*)

Acknowledgements

The offshore data were provided by the Kashima Port Construction Office of the Ministry of Land, Infrastructure, Transport and Tourism, and the Marine Information Division of the Port and Airport Research Institute. All the staff members of HORS are gratefully acknowledged for their contributions to the field measurements.

References

Bailard, J.A. (1981): An energetics total load sediment transport model for a planar sloping beach, *J. Geophys. Res.,* Vol.86, No.C11, pp.10938-10954.

Birkemeier, W.A. (1984): Time scales of nearshore profile changes, *Proc. 19th Int. Conf. Coastal Eng.,* ASCE, pp.1507-1521.

Doering, J.C. and Bowen, A.J. (1995): Parameterization of orbital velocity asymmetries of shoaling and breaking waves using bispectral analysis, *Coastal Eng.,* Vol.26, pp.15-33.

Duan, Q.Y., Gupta, V.K. and Sorooshian, S. (1993): Shuffled complex evolution approach for effective and efficient global minimization, *J. Optimization Theory and Applications*, Vol.73, No.3, pp.501-521.

Gallagher, E.L., Elgar, S. and Guza, R.T. (1998): Observations of sand bar evolution on a natural beach. *J. Geophys. Res.,* Vol.103, No.C2, pp.3203-3215.

Garcez-Faria, A.F., Thornton, E.B., Stanton, T.P., Soares, C.V. and Lippmann, T.C. (1998): Vertical profiles of longshore currents and related bed shear stress and bottom roughness, *J. Geophys. Res.,* Vol.103, No.C2, pp.3217-3232.

Garcez-Faria, A.F., Thornton, E.B., Lippmann, T.C. and Stanton, T.P. (2000): Undertow over a barred beach, *J. Geophys. Res.,* Vol.105, No.C7, pp.16,999-17010.

Goda, Y. (1975): Irregular wave deformation in the surf zone, *Coastal Eng. in Japan*, Vol.18, pp.13-26.

Goda, Y. (1983): A unified nonlinearity parameter of water waves, *Rep. Port and Harbour Res. Inst.,* Vol.22, No.3, pp.3-30.

Goda, Y. (1985): Numerical examination of several statistical parameters of sea waves, *Rep. Port and Harbour Res. Inst.,* Vol.24, No.4, pp.65-102. (in Japanese)

Grasmeijer, B.T. and Ruessink, B.G. (2003): Modeling of waves and currents in the nearshore parametric vs. probabilistic approach, *Coastal Eng.,* Vol.49, pp.185-207.

Grunnet, N.M., Walstra, D.J. and Ruessink, B.G. (2004): Process-based modelling of a shoreface nourishment, *Coastal Eng.,* Vol.51, pp.581-607.

Hashimoto, N., Kawaguchi, K., Maki, T. and Nagai, T. (2000): A comparison of WAM and MRI based on observed directional wave spectra, *Hydrodynamics IV*, Vol. II, ICHD2000 Local Organizing Committee, pp.587-592.

Hoefel, F. and Elgar, S. (2003): Wave-induced sediment transport and sandbar migration, *Science,* Vol.299, pp.1885-1887.

Hsu, T.J., Elgar, S. and Guza, R.T. (2006): Wave-induced sediment transport and onshore sandbar migration, *Coastal Eng.,* Vol.53, pp.817-824.

Katoh, K. and Yanagishima, S. (1995): Changes of sand grain distribution in the surf zone, *Proc. Coastal Dynamics '95*, ASCE, pp.639-650.

Kobayashi, N., Payo, A. and Schmied, L. (2008): Cross-shore suspended sand and bed load transport on beaches, *J. Geophys. Res.,* Vol.113, C07001, doi,10.1029/2007JC004203.

Kuriyama, Y. (1991): Investigation on cross-shore sediment transport rates and flow parameters in the surf zone using field data, *Rep. Port and Harbour Res. Inst.,* Vol.31, No.2, pp.3-58.

Kuriyama, Y. (1996): Models of wave height and fraction of breaking waves on a barred beach, *Proc. 26th Int. Conf. Coastal Eng.,* ASCE, pp.247-260.

Kuriyama, Y. (2002): Medium-term bar behavior and associated sediment transport at Hasaki, Japan, *J. Geophys. Res.,* Vol.107, No.C9, 3132, doi,10.1029/2001JC000899.

Kuriyama, Y. (2010a): One-dimensional model for undertow and longshore current velocities in the surf zone, *Rep. Port and Airport Res. Inst.,* Vol.49, No.2. (in press)

Kuriyama, Y. (2010b): Prediction of cross-shore distribution of longshore sediment transport rate in and outside the surf zone, *Rep. Port and Airport Res. Inst.,* Vol.49, No.2. (in press)

Kuriyama, Y. and Nakatsukasa, T. (2000): A one-dimensional model for undertow and longshore current on a barred beach, *Coastal Eng.,* Vol.40, pp.39-58.

Kuriyama, Y. and Ozaki, Y. (1996): Wave height and fraction of breaking waves on a bar-trough beach -Field measurements at HORS and modeling-, *Rep. Port and Harbour Res. Inst.*, Vol.35, No.1, pp.1-38.

Kuriyama, Y., Katoh, K. and Isogami, T. (1990): Wave nonlinearity and cross-shore sediment transport rate in the vicinity of breaker zone, *Proc. Coastal Eng.,* JSCE, pp.284-260. (in Japanese)

Kuriyama, Y., Ito, Y. and Yanagishima, S. (2008a): Medium-term variations of bar properties and their linkages with environmental factors at Hasaki, Japan, *Mar. Geol.,* Vol.248, pp.1-10, doi,10.1016/j.margeo.2007.10.006.

Kuriyama, Y., Ito, Y. and Yanagishima, S. (2008b): Cross-shore variation of long-term average longshore

current velocity in the nearshore zone, *Continental Shelf Res.,* Vol.28, No.3, pp.491-502, doi,10.1016/ j.csr.2007.10.008.

Lippmann, T.C., Holman, R.A. and Hathaway, K.K. (1993): Episodic, nonstationary behavior of a double bar system at Duck, North Carolina, U.S.A., 1986-1991, *J. Coastal Res.,* SI15, pp.49-75.

Murphy, A.H. and Epstein, E.S. (1989): Skill scores correlation coefficients in model verification, *Monthly Weather Review*, Vol.117, pp.572-581.

Nishimura, H. (1988): Computation of nearshore current, In *Nearshore Dynamics and Coastal Process –Theory, Measurements and Predictive Models-* (edited by Horikawa, K.), University of Tokyo Press, pp.271-291.

Pape, L., Ruessink, B.G., Wiering, M.A. and Turner, I.L. (2007): Recurrent neural network modeling of nearshore sand bar behavior, *Neural Network,* Vol.20, pp.509-518.

Pape, L., Plant, N.G. and Ruessink, B.G. (2009): Cross-shore sandbar response to waves, *J. Coastal Res.,* SI56, pp.1030-1034.

Pape, L. Ruessink, G. and Kuriyama, Y. (2009): Models and scales for nearshore sandbar behavior, *Proc. Coastal Dynamics 2009*, ASCE, CD-ROM.

Plant, N.G., Holman, R.A., Freilich, M.H. and Birkemeier, W.A. (1999): A simple model for interannual sandbar behavior, *J. Geophys. Res.,* Vol.104, No.C7, pp.15755-75776.

Plant, N.G., Ruessink, B.G. and Wijnberg, K.M. (2001): Morphologic properties derived from a simple cross-shore sediment transport model, *J. Geophys. Res.,* Vol.106, No.C1, pp.945-958.

Plant, N.G., Holland, K.T., Puleo, J.A. and Gallagher, E.L. (2004): Prediction skill of nearshore profile evolution models, *J. Geophys. Res.,* Vol.109, C01006, doi,10.1029/ 2003JC001995.

Reniers, A.J.H.M., Thornton, E.B., Stanton, T.P. and Roelvink, J.A. (2004): Vertical flow structure during Sandy Duck, observations and modeling, *Coastal Eng.,* Vol.51, pp.237-260.

Ruessink, B.G. and Kroon, A. (1994): The behavior of a multiple bar system in the nearshore zone of Terschelling, the Netherlands, 1965-1993, *Mar. Geol.,* Vol.121, pp.187-197.

Ruessink, R.A. and Kuriyama, Y. (2008): Numerical predictability experiments of cross-shore sandbar migration, *Geophys. Res. Letter,* Vol.35, L01603, doi,10.1029/ 2007GL032530.

Ruessink B.G., Miles, J.R., Feddersen, F., Guza, R.T. and Elgar, S. (2001): Modeling the alongshore current on barred beaches, *J. Geophys. Res.,* Vol.106, No.C10, pp.22451-22463.

Ruessink, B.G., Wijnberg, K.M., Holman, R.A., Kuriyama, Y. and van Enckevort, I.M.J. (2003): Intersite comparison of interannual nearshore bar behavior, *J. Geophys. Res.,* Vol.108, No.C8, doi,10.1029/ 2002JC001505.

Ruessink, B. G., Kuriyama, Y., Reniers, A. J. H. M., Roelvink, J. A. and Walstra, D. J. R. (2007): Modeling cross-shore sandbar behavior on the timescale of weeks, *J. Geophys. Res.,* Vol.112, F03010, doi,10.1029/ 2006JF000730.

Seyama, A. and Kimura, A. (1988): The measured properties of irregular wave breaking and wave height change after breaking on the slope, *Proc. 21st Int. Conf. Coastal Eng.,* ASCE, pp.419-432.

Shand, R.D. and Bailey, D.G. (1999): A review of net offshore bar migration with photographic illustrations from Wanganui, New Zealand, *J. Coastal Res.,* Vol.15, pp.365-378.

Shand, R.D., Bailey, D.G. and Shepherd, M.J. (1999): An inter-site comparison of net offshore bar migration characteristics and environmental conditions, *J. Coastal Res.,* Vol.15, pp.750-765.

Svendsen, I.A. (1984): Mass flux and undertow in a surf zone, *Coastal Eng.,* Vol.8, pp.347-365.

Thornton, E.B. and Guza, R.T. (1983) Transformation of wave height distribution, *J. Geophys. Res.,* Vol.88, No.C10, pp.5925-5938.

van Rijn, L.C., Walstra, D.J.R., Grasmeijer, B., Sutherland, J., Pan, S. and Sierra, J.P. (2003): The predictability of cross-shore bed evolution of sandy beaches at the time scale of storms and seasons using process-based profile models, *Coastal Eng.,* Vol.47, pp.295-327.

Walstra, D.J. and Ruessink, G. (2009): Process-based modeling of cyclic bar behavior on yearly scales, *Proc. Coastal Dynamics 2009*, ASCE, CD-ROM.

Wijnberg, K.M. and Terwindt, J.H.J. (1995): Extracting decadal morphological behaviour from high-resolution, long-term bathymetric surveys along the Holland coast using eigenfunction analysis, *Mar. Geol.,* Vol.126, pp.301-330

港湾空港技術研究所報告　第 49 巻第 2 号

２０１０．６

編集兼発行人　独立行政法人港湾空港技術研究所

発　行　所　独立行政法人港湾空港技術研究所
横須賀市長瀬３丁目１番１号
TEL. 046(844)5040 URL. http://www.pari.go.jp/

印　刷　所　株式会社　大　應

CONTENTS